Geophysical Research Letters

RESEARCH LETTER
10.1029/2019GL083745

Quantifying the Local Effect of Northern Hemisphere Atmospheric Blocks on the Persistence of Summer Hot and Dry Spells

Matthias Röthlisberger[1,2,3] and **Olivia Martius**[1,2,4]

[1]Institute of Geography, University of Bern, Bern, Switzerland, [2]Oeschger Centre for Climate Change Research, University of Bern, Bern, Switzerland, [3]Institute for Atmospheric and Climate Science, ETH Zürich, Zürich, Switzerland, [4]Mobiliar Lab for Natural Risks, University of Bern, Bern, Switzerland

Key Points:
- Blocks strongly affect the persistence of hot, dry, and compound hot and dry spells occurring colocated with the blocks
- This effect is generally positive for hot spell persistence, while it can take both signs for dry spell persistence
- Strongest positive effect of blocks on compound hot and dry spell persistence is found over western North America and southern Europe

Supporting Information:
- Supporting Information S1

Correspondence to:
M. Röthlisberger,
matthias.roethlisberger@env.ethz.ch

Citation:
Röthlisberger, M., & Martius, O. (2019). Quantifying the local effect of Northern Hemisphere atmospheric blocks on the persistence of summer hot and dry spells. *Geophysical Research Letters*, *46*, 10,101–10,111. https://doi.org/10.1029/2019GL083745

Received 16 MAY 2019
Accepted 5 AUG 2019
Accepted article online 9 AUG 2019
Published online 23 AUG 2019

Abstract The persistence of heat waves and droughts is a key factor in determining their societal impact. Here, the local effect of atmospheric blocks on the persistence of summer hot and dry spells is quantified by comparing their climatological daily survival probability, that is, the probability to survive the next day, to their daily survival probability when they co-occur with a block. The survival odds of hot spells are increased by more than 50% over most of the Northern Hemisphere extratropical land masses when co-occurring with blocks. Dry spell persistence is also strongly increased by colocated blocks over western North America, Europe, and southern Russia, while it is significantly decreased over the western North Atlantic and the western North Pacific. These spatial differences in the effect of blocks on both spell types are explained by considering the spatially varying surface temperature and precipitation anomalies induced by the blocks.

Plain Language Summary The persistence of heat waves and droughts strongly affects how challenging these weather events are to societies. However, the meteorological phenomena that foster the persistence of heat waves and droughts are not yet fully understood. Here we focus on one such meteorological phenomenon, namely, stationary high-pressure systems known as atmospheric blocks, and quantify their effect on the persistence of hot and dry spells that co-occur with the blocks. For hot spells, this effect is positive almost everywhere blocks occur in the Northern Hemisphere, most strongly so over land. Dry spell persistence is also strongly affected by blocks, but the effect can be either positive or negative. Over land, the strongest positive effects of blocks on dry spell persistence are found over western North America, Europe, and southern Russia. There, blocks also increase the persistence of so-called compound hot and dry spells, that is, periods with both hot and dry weather occurring concomitantly. Our results show that changes in the number and geographical distribution of blocks with climate change would significantly affect hot and dry spell persistence in a future climate.

1. Introduction

In the Northern Hemisphere extratropics, several recent long-lasting heat waves such as the European summer heat wave in 2003 and the Russian heat wave in 2010 caused substantial loss of lives and had significant adverse ecological and economic effects (Ciais et al., 2005; Fouillet et al., 2006; García-Herrera et al., 2010; Lesk et al., 2016). Individual hot days may cause discomfort to some people; however, the severest socioeconomic impacts conceivably result from unusually persistent events. While many studies have focused on the magnitude of such extreme events (e.g., Barriopedro et al., 2011; Schär et al., 2004), the persistence of these events is much less studied, despite its fundamental role in generating societal impact.

Drought is a further major societal concern that may arise from unusually persistent surface weather and that can pose serious threats to food security in a warming climate (Kotir, 2011; Porter et al., 2014). Moreover, several recent studies have emphasized the potentially devastating effects of so-called compound heat and drought events (IPCC, 2012; Leonard et al., 2014; Zscheischler & Seneviratne, 2017), that is, periods during which both drought and heat occur concomitantly at the same location. When pondering about future weather related risks, it is therefore important to understand what makes heat waves, droughts, and compound heat and drought conditions particularly persistent.

In the Northern Hemisphere extratropics, different factors are known to contribute to the persistence of heat and drought. For instance, it is well known that heat and drought can re-enforce and prolong each other

through land-atmosphere feedbacks (Fischer et al., 2007; Hirschi et al., 2011; Lorenz et al., 2010; Seneviratne et al., 2010; Zscheischler & Seneviratne, 2017). However, also synoptic to hemispheric-scale atmospheric circulation patterns play a pivotal role in generating long-lasting heat waves and droughts. Recent studies have therefore investigated the atmospheric dynamics mechanisms leading to persistent hot surface weather for several recent examples of extremely long-lasting heat waves (Barriopedro et al., 2011; Black et al., 2004; Dole et al., 2011; Fink et al., 2004; Parker et al., 2014; Schneidereit et al., 2012; Xu et al., 2019; Zschenderlein et al., 2018) as well as from a climatological point of view (Kornhuber et al., 2017; Röthlisberger et al., 2019).

The most widely studied atmospheric process conducive to persistent summer heat and drought is atmospheric blocking (Barriopedro et al., 2011; Black et al., 2004; Drouard & Woollings, 2018; Schaller et al., 2018; Schneidereit et al., 2012). Blocks are stationary anticyclones that block the westerly flow in the midlatitudes (e.g., Barriopedro et al., 2006; Pelly & Hoskins, 2003; Rex, 1950) and thereby induce significant precipitation (Lenggenhager & Martius, 2019; Sousa et al., 2017; Trigo et al., 2004) and temperature anomalies (e.g., Pfahl & Wernli, 2012) in and around the blocked area.

In the upstream (western) part of the block, warm air advection leads to positive surface temperature anomalies, while in the central and downstream (eastern) part of the blocks subsidence leads to adiabatic warming and clear-sky radiative forcing at the surface (Bieli et al., 2015; Pfahl & Wernli, 2012; Woollings et al., 2018). However, in the downstream part of the block, cold air advection occurs (Buehler et al., 2011; Sousa et al., 2018; Whan et al., 2016) and can partly offset the surface warming due to the adiabatic compression and clear-sky radiative forcing. Over land areas, increased solar irradiation in combination with a subsidence-induced precipitation deficit often leads to soil moisture depletion, which further increases surface temperatures due to increased surface sensible heat fluxes (Fischer et al., 2007; Hirschi et al., 2011; Lorenz et al., 2010). Due to the stationarity of blocks, the associated temperature anomalies can be expected to be rather persistent. However, despite clear dynamical arguments and case study evidence for the relevance of blocks in affecting the persistence of heat waves, no study has so far quantified this effect climatologically.

The effect of blocks on wet and dry spell persistence is considerably more complex and spatially more variable, as precipitation anomalies of both signs often occur within a block (e.g., Sousa et al., 2017). The central and downstream part of blocks typically exhibits negative precipitation anomalies due to the aforementioned subsidence (e.g., Sousa et al., 2017). In the upstream and northern part of the block, positive precipitation anomalies and variable weather conditions occur due to a deflection of cyclone tracks by the block (Lenggenhager & Martius, 2019; Sousa et al., 2017; Trigo et al., 2004), conceivably yielding relatively short dry spells there. However, the magnitude and exact location of these precipitation anomalies within the block differ strongly between blocks occurring in different geographical regions (Lenggenhager & Martius, 2019; Sousa et al., 2017). Unlike for hot spells, it is therefore not a priori clear where (and if at all) blocks significantly increase or decrease the persistence of dryness occurring colocated with the block.

Here we quantify the climatological effect of atmospheric blocks on the persistence of both hot and dry spells occurring colocated with Northern Hemisphere blocks. We specifically focus on blocks and spells during the extended summer (May–October, MJJASO). To define and quantify "spell persistence," we follow the approach of Moon et al. (2018) who studied drought persistence based on the survival probability of droughts on monthly and annual time scales. Here we compare the climatological daily survival probabilities of hot and dry spells with their respective daily survival probabilities when they occur colocated with blocks. Thereby, we also assess the spatial variability in the local effect of blocks on the persistence of hot and dry spells. Finally, we extend this analysis to compound hot and dry spells.

2. Data and Methods

2.1. ERA-Interim

For our analyses we use the ERA-Interim reanalysis data set (Dee et al., 2011) for the period 1980–2015. ERA-Interim is produced with a T255 spectral horizontal resolution and 60 hybrid σ-p levels in the vertical. We used ERA-Interim at a 6-hourly temporal resolution and interpolated the data horizontally to a 1° by 1° grid and vertically to pressure levels.

2.2. Hot, Dry, and Compound Hot and Dry Spells

Hot spells are identified in the ERA-Interim data set at each grid point based on daily maxima of the 6-hourly 2-m temperature (hereafter referred to as T2mmax) for the period 1980–2015. First, the data are detrended by removing a linear trend at each grid point. Second, at each grid point and for each calendar day, the 80th percentile of the detrended T2mmax data is calculated. Hot spells are then identified as consecutive hot days, that is, days during which the detrended T2mmax exceeds or is equal to its local calendar day 80th percentile.

Dry spells are identified in ERA-Interim as consecutive days during which the daily accumulated precipitation is below a fixed threshold of 1 mm, without first detrending the data. Finally, compound hot and dry spells are identified as consecutive days, which are both hot and dry. For all spell types all data from leap days are discarded.

These definitions of hot, dry, and compound hot and dry spells result in a binary daily time series $Spell_{g,k}(t)$ at each grid point g and for each spell-type $k \in \{dry,\ hot, compound\}$, indicating spell occurrence (1) and nonspell conditions (0) for each day t.

2.3. Atmospheric Blocks and Surface Cyclones

To identify atmospheric blocking, an updated version of the blocking identification algorithm of Schwierz et al., 2004 is used in this study. This algorithm identifies persistent negative anomalies in the 500 to 150 hPa vertically averaged potential vorticity (PV), which are first calculated relative to the climatological 30-day running mean centered on the day of interest. Then, they are smoothed using a 2-day running mean. Blocking events are identified as spatial objects based on a PV anomaly threshold of –1.0 PVU (1 PVU = 10^{-6} m^2 s^{-1} K kg^{-1}) and then tracked as long as they exhibit a spatial overlap of at least 70% between each 6-hourly time step. These blocks are hence only quasi-stationary and on average propagate northeastward during their life cycle (Croci-Maspoli et al., 2007). Furthermore, a minimum lifetime criterion of 5 days is imposed. Note that the PV anomaly threshold used here is between the thresholds for strong (−1.3 PVU) and weak (−0.7 PVU) blocks proposed in Pfahl and Wernli (2012). Atmospheric blocking events are calculated at 6-hourly temporal resolution and then aggregated to a binary daily time series $B_g(t)$ for each grid point g, which takes the value 1 for all days t during which a block occurs at least at one 6-hourly time step of that day at grid point g, and 0 otherwise.

Further, we use an objective extratropical cyclone identification algorithm (described in detail in Wernli & Schwierz, 2006 and Sprenger et al., 2017), which identifies and tracks surface cyclones as closed sea level pressure contours that encompass a local sea level pressure minimum.

2.4. Survival Probabilities

Here we focus on hot, dry, and compound hot and dry spells during the extended summer (MJJASO) as opposed to the classical summer months July–August in order to maximize the sample size available for our statistical analyses. We thus introduce a dummy variable $m(t)$ that takes the value 1 if the day t belongs to MJJASO and 0 otherwise. The climatological persistence of k-type spells during MJJASO at grid point g can then be quantified from $Spell_{g,k}(t)$ by calculating the climatological (daily) survival probability of k-type spells ($Pss_{g,k}$) as

$$Pss_{g,k} = \mathrm{P}\Big(Spell_{g,k}(t+1) = 1 \mid Spell_{g,k}(t) = 1 \wedge m(t) = 1\Big).$$

To assess the effect of atmospheric blocks on the spell persistence, the survival probability of k-type spells during colocated blocks is calculated as

$$Pss^{b}_{g,k} = \mathrm{P}\Big(Spell_{g,k}(t+1) = 1 \mid Spell_{g,k}(t) = 1 \wedge B_g(t) = 1 \wedge m(t) = 1\Big).$$

The number of days available for computing $Pss_{g,k}$ and $Pss^{b}_{g,k}$ for $k \in \{hot, dry, compound\}$ is shown in Figures S1 and S2 in the supporting information. In a next step, the odds of spell survival during colocated blocking events $O^{b}_{g,k} = Pss^{b}_{g,k}/\left(1-Pss^{b}_{g,k}\right)$ are compared to the climatological survival odds $O_{g,k} = Pss_{g,k}/(1 - Pss_{g,k})$ by calculating the odds ratio as

$$\mathrm{OR}_{\mathrm{g,k}} = \frac{\mathrm{O}^{\mathrm{b}}_{\mathrm{g,k}}}{\mathrm{O}_{\mathrm{g,k}}} = \frac{\mathrm{Pss}^{\mathrm{b}}_{\mathrm{g,k}}\left(1-\mathrm{Pss}_{\mathrm{g,k}}\right)}{\left(1-\mathrm{Pss}^{\mathrm{b}}_{\mathrm{g,k}}\right)\mathrm{Pss}_{\mathrm{g,k}}}.$$

The value of $OR_{g,k}$ indicates how the odds of spell survival change when a block is present at the same grid point, that is, if $OR_{g,k} > 1$ ($OR_{g,k} < 1$) blocks are associated with an increase (decrease) in the odds of spell survival of k-type spells at grid point g and thus increased (decreased) spell persistence. Note that the causality implied here is not proven directly by our statistical analyses. Rather, it derives from the large body of literature that has illustrated the causality between atmospheric blocks and their effects on surface weather (see references in section 1).

The statistical significance of $OR_{g,k}$ is assessed using a bootstrapping method in close analogy to that used in Röthlisberger et al. (2016). First, 1,000 synthetic blocking time series $B^r_g(t)$ are constructed by shuffling randomly the 36 annual chunks of $B_g(t)$. Then, 1,000 synthetic $Pss^b_{g,k}$ values ($Pss^{b,r}_{g,k}$) are calculated as

$$Pss^{b,r}_{g,k} = \mathrm{P}\left(Spell_{g,k}(t+1) = 1 \mid Spell_{g,k}(t) = 1 \wedge B^r_g(t) = 1 \wedge m(t) = 1\right)$$

and subsequently used to derive synthetic $OR_{g,k}$ values ($OR^r_{g,k}$):

$$\mathrm{OR}^{\mathrm{r}}_{\mathrm{g,k}} = \frac{\mathrm{Pss}^{\mathrm{b,r}}_{\mathrm{g,k}}\left(1-\mathrm{Pss}_{\mathrm{g,k}}\right)}{\left(1-\mathrm{Pss}^{\mathrm{b,r}}_{\mathrm{g,k}}\right)\mathrm{Pss}_{\mathrm{g,k}}}.$$

Hereby, shuffling all annual chunks of $B_g(t)$ ensures that the blocking frequency in all $B^r_g(t)$ equals that of $B_g(t)$ and, moreover, makes sure that seasonal variations in the blocking frequency and in the spell persistence do not affect our results. Statistical significance is then assigned to a particular $OR_{g,k}$ value in a two-step approach exactly as in Röthlisberger et al. (2016): First, a p value for each $\mathrm{OR}_{g,k}$ value is estimated by comparing it to the respective 1,000 $OR^r_{g,k}$ values. Note that a p value of 0 is assigned to an $OR_{g,k}$ value if the $OR_{g,k}$ value is outside the range of the $OR^r_{g,k}$ values. Second, the false discovery rate test of Benjamini and Hochberg (1995) is applied to the resulting field of p values. Following Wilks (2016), we use a maximum false discovery rate of 0.1.

Three points regarding our methodology should be kept in mind. First, the threshold for identifying hot spells is slightly lower than that used in other studies (Brunner et al., 2018; Sillmann et al., 2013). However, the average T2mmax anomaly during hot spells defined by our approach ranges from +4 to +7 K over most land areas (Figure S3), which illustrates that these periods are indeed rather hot.

Second, we quantify spell persistence based on the spell survival probability and not based on the spell durations. This is highly beneficial for addressing the research question of this study because there are numerous spells that only partially coexist with blocks. When assessing the effect of blocks on spell durations, it is necessary to determine for each spell whether or not it is affected by a block. For spells only partially coexisting with blocks, a subjective overlap criterion is required. In our approach, no such subjectivity is necessary, as survival probabilities are calculated by considering the individual time steps, during each of which coexistence of spells and blocks is well defined. Therefore, $OR_{g,k}$ is a more objective measure of the effect of blocks on spell persistence than changes in any statistical measure of the spell duration distribution.

Third, similar to Furrer et al. (2010) and Moon et al. (2018) no subjective minimum duration criterion is used for identifying spells. Rather, a period of any length during which a certain spell criterion is met is considered as a spell, which is consistent with focusing on spell survival probabilities rather than durations.

3. Results

The climatological survival probability of hot spells ($Pss_{g,hot}$) reaches values of up to 0.75 over the Arctic Ocean, Greenland, as well as in the North Sea (Figure 1a). In the midlatitudes $Pss_{g,hot}$ values range from roughly 0.5 to 0.65, with lower values over the central North Pacific and western North Atlantic. While

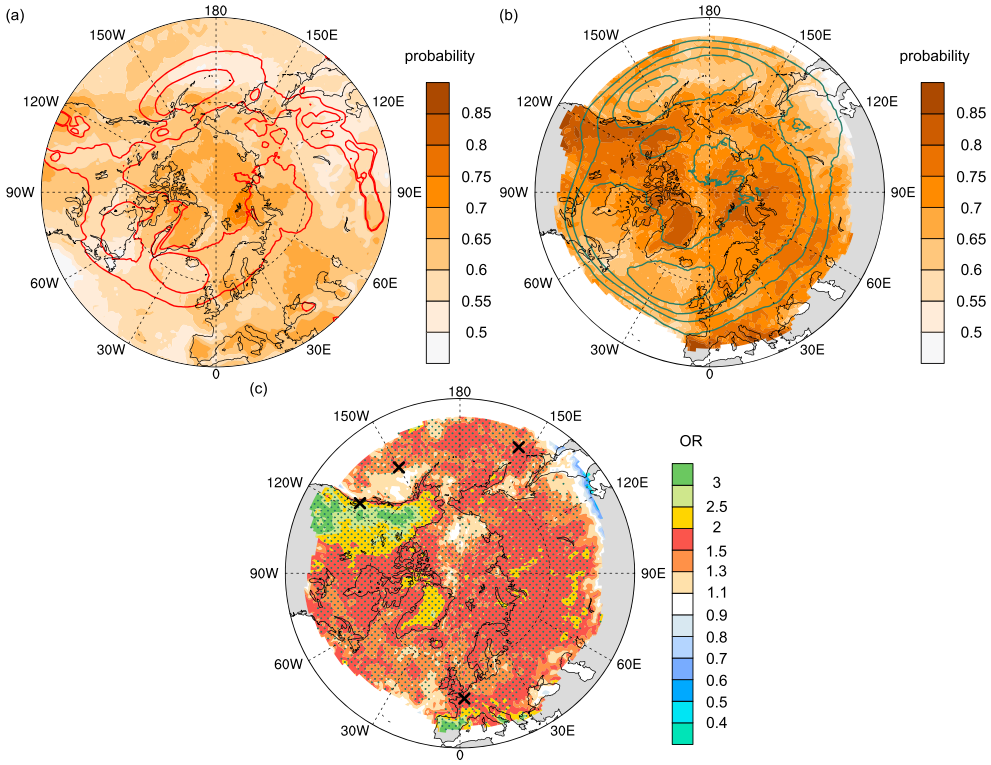

Figure 1. Results for hot spells. (a) Climatological May–October (MJJASO) hot spell survival probabilities ($Pss_{g,hot}$) and (b) survival probabilities of MJJASO hot spells during colocated blocks ($Pss^{b}_{g,hot}$). Red contours in (a) show MJJASO cyclone frequencies of 30% and 40%, respectively, and green contours in panel (b) depict MJJASO blocking frequencies (number of blocked days divided by total number of MJJASO days) of 5%, 10%, 15%, and 20%. (c) Odds ratios for MJJASO hot spells ($OR_{g,hot}$). Stippling indicates odds ratios statistically significantly different from 1. In panels (b) and (c) values are only plotted in areas where at least 50 days were available to compute $Pss^{b}_{g,hot}$. Black crosses in (c) indicate the grid points for which composites are shown in Figure 3.

the exact $Pss_{g,hot}$ values depend on the definition of hot spells, Figure 1a illustrates the spatial variability in the climatological persistence of summer hot spells in the Northern Hemisphere extratropics.

Hot spell survival probabilities conditional to the occurrence of colocated blocks ($Pss^{b}_{g,hot}$) are larger than their climatological values in most places where blocks occur (Figures 1a and 1b). Consequently, the resulting odds ratios ($OR_{g,hot}$) are statistically significantly larger than one in most areas of the Northern Hemisphere extratropics, in particular over land (Figure 1c). The land-sea contrast in $OR_{g,hot}$ is particularly well visible at the west coast of Canada. The largest $OR_{g,hot}$ values are found over the northwestern United States and western Canada as well as parts of southern Europe, where the odds of hot spell survival are more than tripled compared to climatology, when a block co-occurs with the spell (Figure 1c). Note, however, that in these regions, blocks do not occur very frequently compared to the blocking hot spots over the North Atlantic and North Pacific (Figure 1b). Thus, during the rare occurrence of a block in these regions with largest statistically significant $OR_{g,hot}$ values, hot spells are particularly likely to persist.

The $Pss_{g,dry}$ field exhibits a markedly different spatial structure than the $Pss_{g,hot}$ field (cf. Figures 1a and 2a). The $Pss_{g,dry}$ values approach 1 in the climatologically driest regions, for example, in central Asia or off the coast of California. Smallest $Pss_{g,dry}$ values are found in the southern and central parts of the North Pacific and North Atlantic storm tracks, Japan, Alaska, and some areas of elevated topography (Figure 2a). Note that the exact $Pss_{g,dry}$ values strongly depend on our definition of dryness, as in dry areas the (absolute) threshold of 1 mm/day accumulated precipitation is exceeded less often than in wetter regions.

In contrast to hot spells, the survival probability of dry spells is not increased everywhere when a block co-occurs with the spell (Figure 2c). The resulting $OR_{g,dry}$ pattern (Figure 2e) is thus more complex but

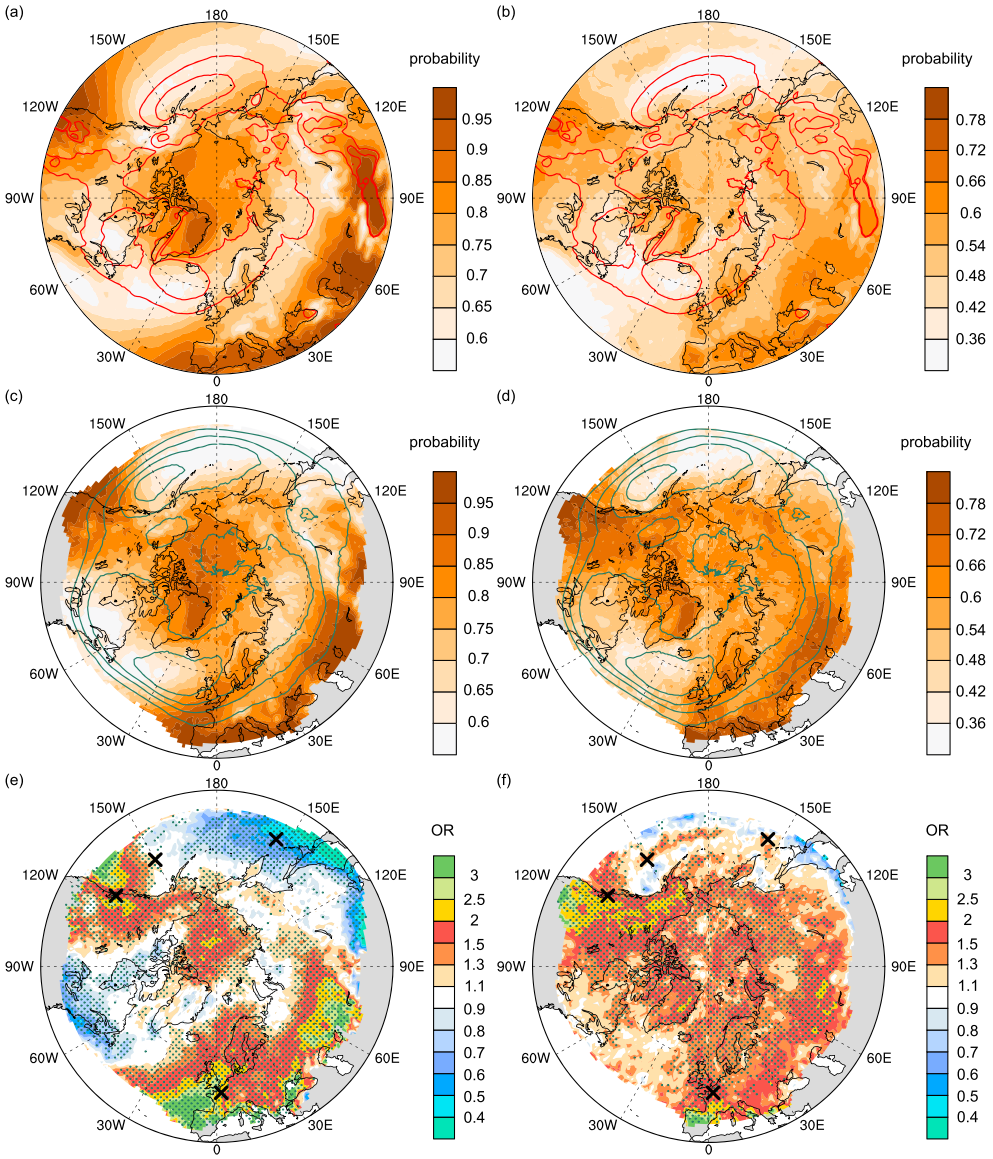

Figure 2. As Figure 1 but for dry spells (left column) and compound dry and hot spells (right column, note the different color scales in the two columns). Panels (a) and (b) depict the climatological survival probabilities $Pss_{g,dry}$ and $Pss_{g,compound}$, (c) and (d) show $Pss^{b}_{g,dry}$ and $Pss^{b}_{g,compound}$, and (e) and (f) depict $OR_{g,dry}$ and $OR_{g,compound}$. Red and green contours in (a)–(d) as in Figures 1a and 1b, stippling in panels (e) and (f) as in Figure 1c but for the respective spell type. Black crosses in (e) and (f) indicate the grid points for which composites are shown in Figure 3. In panels (cf) values are only shown where more than 50 days were available to compute the respective $Pss^{b}_{g,k}$.

nevertheless reveals very clear spatial structures of statistically significant odds ratios. Dry spell persistence is markedly increased during blocks in particular over southern North America, the eastern North Atlantic and Europe, and western Russia. In these areas, $OR_{g,dry}$ values exceed three in some areas, implying a threefold increase in the odds of dry spell survival when a block is present at the same grid point. However, over the western North Atlantic and western North Pacific, $OR_{g,dry}$ values below 0.5 are found in some areas, which indicates that in these regions, the odds of dry spell survival are more than halved compared to climatology when a block occurs there. Note, however, that also in these regions with $OR_{g,dry} < 1$, blocks occur quite rarely (Figures 2c and 2e) and thus their negative effect on dry spell persistence does not manifest itself very frequently.

The spatial variability in the climatological survival probability of compound dry and hot spells ($Pss_{g,compound}$) is similar to that of hot spells (Figures 1a and 2b), but $Pss_{g,compound}$ is slightly smaller than $Pss_{g,hot}$

at all grid points, due to the additional constraint of dryness for compound spells. The $OR_{g,compound}$ field combines features from both the $OR_{g,hot}$ and $OR_{g,dry}$ fields and exhibits $OR_{g,compound}$ values statistically significantly larger than 1 over western North America, western Europe, southern Russia, and parts of the Arctic (Figure 2f). However, over the North Pacific and the North Atlantic, blocks have no local effect on compound dry and hot spell survival (Figure 2f).

4. Discussion

The $OR_{g,hot}$ field reveals that blocks have a very clear and statistically significant positive effect on the persistence of hot spells occurring colocated with the block, as the odds of hot spell survival are increased by more than 50% ($OR_{g,hot} > 1.5$) over almost the entire extratropical Northern Hemisphere land masses. Also, over the oceans blocks significantly increase the survival probability of colocated hot spells, albeit less strongly. This generally positive local effect of blocks on hot spell persistence was anticipated from the literature discussed in section 1. The novel aspects of this study are the quantification of this effect, as well as the assessment of the spatial variability in its strength.

The $OR_{g,hot}$ field reveals that in particular, western North America and parts of Europe are most susceptible to blocking-induced persistent summer heat. Furthermore, a clear land-sea contrast in the local effect of blocks on hot spell persistence is apparent in the $OR_{g,hot}$ field, for example, across the North American west coast. On the one hand, this land-sea contrast arises from the larger thermal inertia of the ocean surface compared to land surfaces, which lets surface air temperatures over the oceans respond much more slowly to an atmospheric temperature forcing than over land (Pfahl & Wernli, 2012). On the other hand, over land areas the soil moisture-atmosphere feedback (e.g., Fischer et al., 2007; Lorenz et al., 2010; Seneviratne et al., 2010) further increases the warm anomalies also in the central and downstream part of the blocks. These two points are illustrated exemplarily for the grid point at 125°W/50°N (Figure 3e), where blocks are associated with a stronger positive T2m anomaly over North American land areas than the adjacent ocean, despite the fact that the anomalies over land are located in the downstream part of blocks, where cold air advection is likely to occur. The land-sea contrast apparent in the $OR_{g,hot}$ field thus further underlines the pivotal role of land surface-atmosphere interactions in amplifying persistent heat (e.g., Lorenz et al., 2010).

The $OR_{g,dry}$ field exhibits a more complex spatial structure than the $OR_{g,hot}$ field, which reflects the more complex effects of blocks on precipitation than on surface temperature. As stated previously, precipitation anomalies of both signs occur within blocks, and the magnitude and exact location of these precipitation anomalies within blocks differ strongly between geographical regions (Lenggenhager & Martius, 2019; Sousa et al., 2017). Major features in the $OR_{g,dry}$ field are thus affected by (a) the regionally differing effects of blocks on precipitation and (b) the climatological distribution of blocking occurrence, which determines whether a particular grid point is located preferentially in the upstream, central, or downstream part of blocks. The interplay between these two factors in modulating $OR_{g,dry}$ is next illustrated exemplarily by showing composites of various variables for days on which blocks occur at selected grid points. Note that during such blocked days, the respective grid point can be located anywhere within the block.

The western North Pacific is a region that is characterized climatologically by a straight and zonal upper level jet (e.g., Koch et al., 2006; Röthlisberger et al., 2018). Blocks occurring at 155°E/45°N (Figure 2c) thus deflects cyclone tracks northward, leading to positive cyclone frequency anomalies and substantial precipitation anomalies in the upstream part of these blocks (Figure 3a). Hereby, the positive precipitation anomalies also reach 155°E/45°N. This indicates that during blocks at 155°E/45°N, precipitation associated with the northward-deflected cyclones frequently reaches this grid point and shortens dry spells there.

At the grid point 150°W/50°N, which is right in the center of the North Pacific blocking frequency maximum, blocks have no statistically significant effect on the persistence of colocated dry spells (Figure 2e). Nevertheless, blocks at this grid point are also associated with positive precipitation anomalies in their upstream part and negative anomalies in the downstream part (Figures 3c and 3d). However, due to its location right in the center of the North Pacific blocking frequency maximum, this grid point is not preferentially located in either the upstream or downstream part of these blocks. Consequently, the reduction in dry spell persistence due to occasional precipitation from the deflected cyclones (when this grid point is located in the upstream part of a block) is balanced by increased dry spell persistence due to subsidence (when this grid

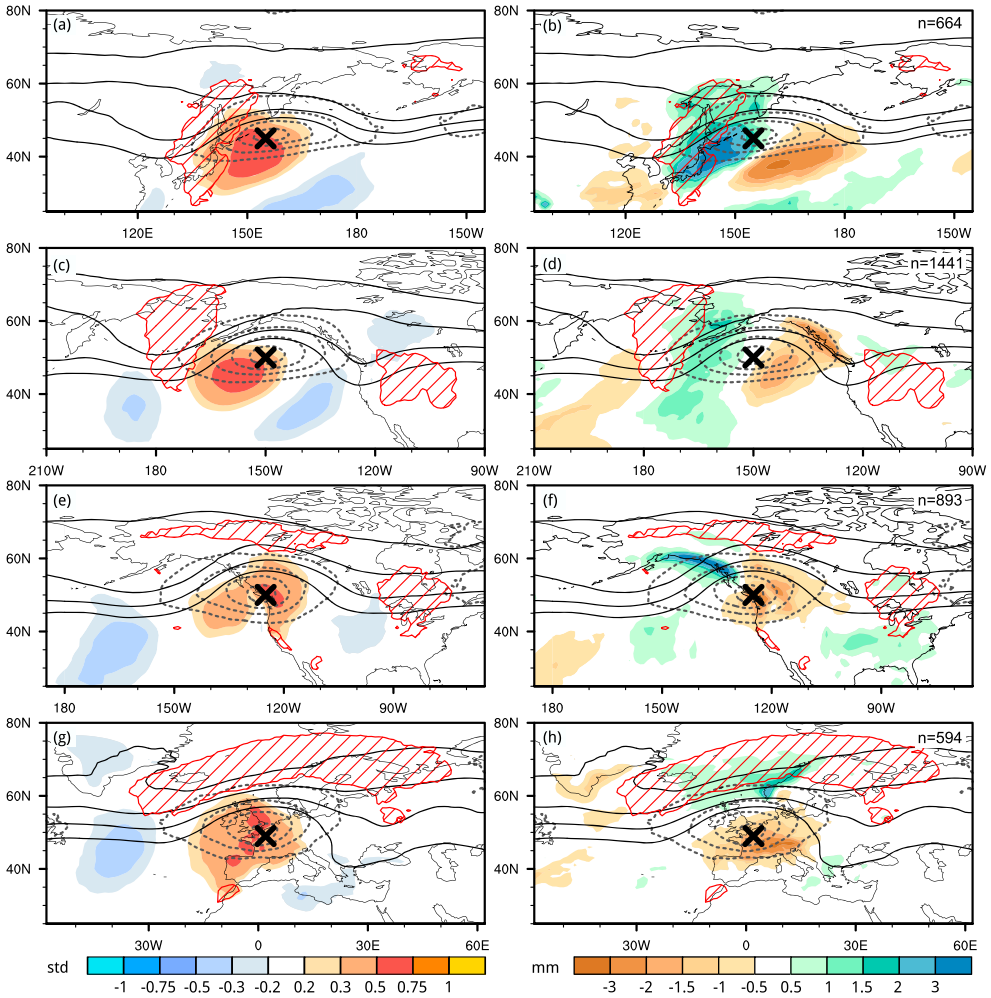

Figure 3. Composites of atmospheric variables for days during which atmospheric blocking occurs at 155°E, 45°N (a and b), 150°W, 50°N (c and d), 125°W, 50°N (e and f), and 2°E and 49°N (g and h, black crosses). Panels (a), (c), (f), and (g) show standardized T2m anomalies (shading), standardized with the local calendar day mean and standard deviation, and (b), (d), (e), and (h) show total precipitation anomaly (relative to the local calendar day mean, in shading). In all panels, black contours depict 400- to 150-hPa vertically averaged potential vorticity (2, 2.5, 3 and 3.5 PVU), gray dashed contours show blocking frequencies (0.2, 0.4, 0.6, and 0.8), and red hatching indicates positive cyclone frequency anomalies exceeding 6 percentage points (relative to the local calendar day mean). The number of days used for the compositing is indicated in the top right of panels (b), (d), (f), and (h).

point is located in the downstream part of a block), yielding no statistically significant climatological effect of blocks on colocated dry spells.

In contrast, blocks at 125°W/50°N and 2°E/49°N lead to a strong northward deflection of cyclones, which induces positive precipitation anomalies primarily to the north of the blocks rather than in their upstream part (Figures 3f and 3h). Consequently, these two grid points are located well within the subsidence-induced negative precipitation anomalies, which explains the strongly positive effect of blocks on dry spell persistence at these grid points.

The findings of our study are somewhat limited by data quality, as ERA-Interim precipitation is not an assimilated variable but rather results from short term model forecasts that have been used to generate ERA-Interim (Dee et al., 2011). Precipitation forecast errors could thus affect dry spell persistence. We have therefore repeated our analysis for dry spells using the satellite-based observational CMORPH data set (Joyce et al., 2004) for the period 2003–2015 (Figure S4). This additional analysis supports our conclusions and reveals a very similar $OR_{g,dry}$ pattern also for this data set, even though the exact $OR_{g,dry}$ values differ

from those shown in Figure 2e. Moreover, fewer $OR_{g,dry}$ values are significantly different from 1, which may be partly due to the shorter time period covered by CMORPH compared to ERA-Interim, yielding fewer spells and blocks available for the statistical analysis.

5. Summary and Conclusions

In this study we quantify the local effect of atmospheric blocks on the persistence of hot, dry, and compound hot and dry spells climatologically and assess the spatial variability in the strength of this effect. This is achieved by comparing the climatological daily survival probability of a particular spell type $k \in \{dry, hot, compound\}$ with the daily survival probability of k-type spells co-occurring with a block at each grid point in the Northern Hemisphere.

It is found that blocks have a significant positive effect on the persistence of colocated hot spells over almost the entire Northern Hemisphere land masses and the survival odds of hot spells are increased by more than 50% (up to 200% in some areas) when a block co-occurs with the spells compared to climatology. The positive effect of blocks on hot spell persistence results from generally positive surface temperature anomalies occurring in all parts of summer blocks (Pfahl & Wernli, 2012). Over land these positive temperature anomalies can be further enhanced by land-atmosphere interactions (Lorenz et al., 2010), which yields a considerable land-sea contrast in the $OR_{g,hot}$ field.

The spatial pattern in the $OR_{g,dry}$ field reveals that blocks positively affect the persistence of colocated dry spells over northwestern North America, Europe, and large parts of Russia with odds ratios exceeding 3 in some areas. Over the western and central North Pacific and the western North Atlantic, blocks negatively affect the persistence of colocated dry spells, with odds ratios below 0.5 in some areas. Composite analyses for several grid points help to understand major features in the $OR_{g,dry}$ field. We conclude that blocks have a strong effect on dry spell persistence; however, it differs across space in both magnitude and sign due to the complex effects of blocks on precipitation, which vary within individual blocks and between blocks in different geographical regions.

The results for compound hot and dry spells are a combination of those for hot and dry spells and reveal that in particular over western North America, western Europe, and southern Russia, compound hot and dry spells are significantly more persistent during colocated blocks. These regions can thus be considered as hot spots for long-lasting compound hot and dry spells associated with blocking. Interestingly, western North America and central Europe are also areas where recurrent Rossby wave patterns (RRWPs) foster particularly long-lasting summer hot spells (Röthlisberger et al., 2019). These areas might thus be particularly prone to persistent heat induced by both blocks and RRWPs. The exact role of and the interplay between RRWPs and blocks in fostering persistent heat (and possibly compound heat and dryness) in these regions remains to be investigated.

The regional differences in the local effect of blocks on hot, dry, and compound hot and dry spell persistence illustrated here are highly relevant for projections of future hot and dry spell persistence. Positive (negative) blocking trends can be expected to lead to colocated positive (negative) trends in hot spell persistence, most strongly so over land areas. Moreover, geographical shifts of the major blocking hot spots (e.g., Dunn-Sigouin & Son, 2013; Masato et al., 2013; Woollings et al., 2018) would conceivably alter the areas in which dry (and compound dry and hot) spell persistence is most strongly affected by blocks. Consequently, trends as well as geographical shifts in blocking occurrence need to be better constrained by future research, as they have the potential to significantly alter hot, dry, and compound hot and dry spell persistence over large land areas in a future climate.

Acknowledgments
The authors acknowledge the Swiss National Science Foundation for funding (Grant 18-255) and two anonymous reviewers for their thoughtful reviews. ERA-Interim data can be accessed online (under http://apps.ecmwf.int/datasets/data/interim-full-daily).

References

Barriopedro, D., Fischer, E., Luterbacher, J., Trigo, R., & Ricardo, G.-H. (2011). The hot summer of 2010: Redrawing the temperature record map of Europe. *Science*, *332*, 220–224. https://doi.org/10.1126/science.1201224

Barriopedro, D., García-Herrera, R., Lupo, A. R., Hernández, E., Barriopedro, D., García-Herrera, R., et al. (2006). A climatology of Northern Hemisphere blocking. *Journal of Climate*, *19*(6), 1042–1063. https://doi.org/10.1175/JCLI3678.1

Benjamini, Y., & Hochberg, Y. (1995). Controlling the false discovery rate: A practical and powerful approach to multiple testing. *Journal of the Royal Statistical Society*, *57*(1), 289–300. https://doi.org/10.1111/j.2517-6161.1995.tb02031.x

Bieli, M., Pfahl, S., & Wernli, H. (2015). A Lagrangian investigation of hot and cold temperature extremes in Europe. *Quarterly Journal of the Royal Meteorological Society*, *141*(686), 98–108. https://doi.org/10.1002/qj.2339

Black, E., Blackburn, M., Harrison, R. G., Hoskins, B. J., & Methven, J. (2004). Factors contributing to the summer 2003 European heatwave. *Weather*, *59*, 217–223. https://doi.org/10.1256/wea.74.04

Brunner, L., Schaller, N., Anstey, J., Sillmann, J., & Steiner, A. K. (2018). Dependence of present and future European temperature extremes on the location of atmospheric blocking. *Geophysical Research Letters*, *45*, 6311–6320. https://doi.org/10.1029/2018GL077837

Buehler, T., Raible, C. C., & Stocker, T. F. (2011). The relationship of winter season North Atlantic blocking frequencies to extreme cold or dry spells in the ERA-40. *Tellus, A: Dynamic Meteorology and Oceanography*, *63*, 174–187. https://doi.org/10.1111/j.1600-0870.2010.00492.x

Ciais, P., Reichstein, M., Viovy, N., Granier, A., Ogée, J., Allard, V., et al. (2005). Europe-wide reduction in primary productivity caused by the heat and drought in 2003. *Nature*, *437*(7058), 529–533. https://doi.org/10.1038/nature03972

Croci-Maspoli, M., Schwierz, C., & Davies, H. C. (2007). A multifaceted climatology of atmospheric blocking and its recent linear trend. *Journal of Climate*, *20*(4), 633–649. https://doi.org/10.1175/JCLI4029.1

Dee, D. P., Uppala, S. M., Simmons, A. J., Berrisford, P., Poli, P., Kobayashi, S., et al. (2011). The ERA-Interim reanalysis: Configuration and performance of the data assimilation system. *Quarterly Journal of the Royal Meteorological Society*, *137*(656), 553–597. https://doi.org/10.1002/qj.828

Dole, R., Hoerling, M., Perlwitz, J., Eischeid, J., Pegion, P., Zhang, T., et al. (2011). Was there a basis for anticipating the 2010 Russian heat wave? *Geophysical Research Letters*, *38*, L06702. https://doi.org/10.1029/2010GL046582

Drouard, M., & Woollings, T. (2018). Contrasting mechanisms of summer blocking over western Eurasia. *Geophysical Research Letters*, *45*(21), 12,040–12,048. https://doi.org/10.1029/2018GL079894

Dunn-Sigouin, E., & Son, S. W. (2013). Northern Hemisphere blocking frequency and duration in the CMIP5 models. *Journal of Geophysical Research: Atmospheres*, *118*, 1179–1188. https://doi.org/10.1002/jgrd.50143

Fink, A. H., Brücher, T., Krüger, A., Leckebusch, G. C., Pinto, J. G., & Ulbrich, U. (2004). The 2003 European summer heatwaves and drought-synoptic diagnosis and impacts. *Weather*, *59*, 209–216. https://doi.org/10.1256/wea.73.04

Fischer, E. M., Seneviratne, S. I., Vidale, P. L., Lüthi, D., & Schär, C. (2007). Soil moisture-atmosphere interactions during the 2003 European summer heat wave. *Journal of Climate*, *20*(20), 5081–5099. https://doi.org/10.1175/JCLI4288.1

Fouillet, A., Rey, G., Laurent, F., Pavillon, G., Bellec, S., Guihenneuc-Jouyaux, C., et al. (2006). Excess mortality related to the August 2003 heat wave in France. *International Archives of Occupational and Environmental Health*, *80*(1), 16–24. https://doi.org/10.1007/s00420-006-0089-4

Furrer, E., Katz, R., Walter, M., & Furrer, R. (2010). Statistical modeling of hot spells and heat waves. *Climate Research*, *43*(3), 191–205. https://doi.org/10.3354/cr00924

García-Herrera, R., Díaz, J., Trigo, R. M., Luterbacher, J., & Fischer, E. M. (2010). A review of the European summer heat wave of 2003. *Critical Reviews in Environmental Science and Technology*, *40*(4), 267–306. https://doi.org/10.1080/10643380802238137

Hirschi, M., Seneviratne, S. I., Alexandrov, V., Boberg, F., Boroneant, C., Christensen, O. B., et al. (2011). Observational evidence for soil-moisture impact on hot extremes in southeastern Europe. *Nature Geoscience*, *4*(1), 17–21. https://doi.org/10.1038/ngeo1032

IPCC (2012). In C. B. Field, V. Barros, T. F. Stocker, D. Qin, D. J. Dokken, K. L. Ebi, et al. (Eds.), *Managing the risks of extreme events and disasters to advance climate change adaptation. A special report of working groups I and II of the intergovernmental panel on climate change*. Cambridge, UK and New York: Cambridge University Press.

Joyce, R. J., Janowiak, J. E., Arkin, P. A., Xie, P., Joyce, R. J., Janowiak, J. E., et al. (2004). CMORPH: A method that produces global precipitation estimates from passive microwave and infrared data at high spatial and temporal resolution. *Journal of Hydrometeorology*, *5*, 487–503. https://doi.org/10.1175/1525-7541(2004)005<0487:CAMTPG>2.0.CO;2

Koch, P., Wernli, H., & Davies, H. C. (2006). An event-based jet-stream climatology and typology. *International Journal of Climatology*, *26*(3), 283–301. https://doi.org/10.1002/joc.1255

Kornhuber, K., Petoukhov, V., Petri, S., Rahmstorf, S., & Coumou, D. (2017). Evidence for wave resonance as a key mechanism for generating high-amplitude quasi-stationary waves in boreal summer. *Climate Dynamics*, *49*(5–6), 1961–1979. https://doi.org/10.1007/s00382-016-3399-6

Kotir, J. H. (2011). Climate change and variability in Sub-Saharan Africa: A review of current and future trends and impacts on agriculture and food security. *Environment, Development and Sustainability*, *13*(3), 587–605. https://doi.org/10.1007/s10668-010-9278-0

Lenggenhager, S., & Martius, O. (2019). Atmospheric blocks modulate the odds of heavy precipitation events in Europe. *Climate Dynamics*. https://doi.org/10.1007/s00382-019-04779-0

Leonard, M., Westra, S., Phatak, A., Lambert, M., van den Hurk, B., McInnes, K., et al. (2014). A compound event framework for understanding extreme impacts. *Wiley Interdisciplinary Reviews: Climate Change*, *5*(1), 113–128. https://doi.org/10.1002/wcc.252

Lesk, C., Rowhani, P., & Ramankutty, N. (2016). Influence of extreme weather disasters on global crop production. *Nature*, *529*(7584), 84–87. https://doi.org/10.1038/nature16467

Lorenz, R., Jaeger, E. B., & Seneviratne, S. I. (2010). Persistence of heat waves and its link to soil moisture memory. *Geophysical Research Letters*, *37*, L09703. https://doi.org/10.1029/2010GL042764

Masato, G., Hoskins, B. J., & Woollings, T. (2013). Winter and summer Northern Hemisphere blocking in CMIP5 models. *Journal of Climate*, *26*(18), 7044–7059. https://doi.org/10.1175/JCLI-D-12-00466.1

Moon, H., Gudmundsson, L., & Seneviratne, S. I. (2018). Drought persistence errors in global climate models. *Journal of Geophysical Research: Atmospheres*, *123*, 3483–3496. https://doi.org/10.1002/2017JD027577

Parker, T. J., Berry, G. J., & Reeder, M. J. (2014). The structure and evolution of heat waves in southeastern Australia. *Journal of Climate*, *27*, 5768–5785. https://doi.org/10.1175/JCLI-D-13-00740.1

Pelly, J. L., & Hoskins, B. J. (2003). A new perspective on blocking. *Journal of the Atmospheric Sciences*, *60*(5), 743–755. https://doi.org/10.1175/1520-0469(2003)060<0743:ANPOB>2.0.CO;2

Pfahl, S., & Wernli, H. (2012). Quantifying the relevance of atmospheric blocking for co-located temperature extremes in the Northern Hemisphere on (sub-)daily time scales. *Geophysical Research Letters*, *39*, L12807. https://doi.org/10.1029/2012GL052261

Porter, J. R., Xie, L., Challinor, A. J., Cochrane, K., Howden, S. M., Iqbal, M. M., et al. (2014). Food security and food production systems. In *Climate Change 2014: Impacts, adaptation, and vulnerability. Part A: Global and sectoral aspects. Contribution of Working Group II to the Fifth Assessment Report of the Intergovernmental Panel on Climate Chan* (Chap. 7, pp. 485–533). Cambridge, UK and New York: Cambridge University Press.

Rex, D. F. (1950). Blocking action in the middle troposphere and its effect upon regional climate. *Tellus*, *2*(3), 196–211. https://doi.org/10.1111/j.2153-3490.1950.tb00331.x

Röthlisberger, M., Frossard, L., Bosart, L. F., Keyser, D., & Martius, O. (2019). Recurrent synoptic-scale Rossby wave patterns and their effect on the persistence of cold and hot spells. *Journal of Climate*, *32*(11), 3207–3226. https://doi.org/10.1175/JCLI-D-18-0664.1

Röthlisberger, M., Martius, O., & Wernli, H. (2018). Northern Hemisphere Rossby wave initiation events on the extratropical jet—A climatological analysis. *Journal of Climate*, *31*(2), 743–760. https://doi.org/10.1175/JCLI-D-17-0346.1

Röthlisberger, M., Pfahl, S., & Martius, O. (2016). Regional-scale jet waviness modulates the occurrence of midlatitude weather extremes. *Geophysical Research Letters*, *43*, 10,989–10,997. https://doi.org/10.1002/2016GL070944

Schaller, N., Sillmann, J., Anstey, J., Fischer, E. M., Grams, C. M., & Russo, S. (2018). Influence of blocking on Northern European and Western Russian heatwaves in large climate model ensembles. *Environmental Research Letters*, *13*. https://doi.org/10.1088/1748-9326/aaba55

Schär, C., Vidale, P. L., Lüthi, D., Frei, C., Häberli, C., Liniger, M. A., & Appenzeller, C. (2004). The role of increasing temperature variability in European summer heatwaves. *Nature*, *427*(6972), 332–336. https://doi.org/10.1038/nature02300

Schneidereit, A., Schubert, S., Vargin, P., Lunkeit, F., Zhu, X., Peters, D. H. W., & Fraedrich, K. (2012). Large-scale flow and the long-lasting blocking high over Russia: Summer 2010. *Monthly Weather Review*, *140*(9), 2967–2981. https://doi.org/10.1175/MWR-D-11-00249.1

Schwierz, C., Croci-Maspoli, M., & Davies, H. C. (2004). Perspicacious indicators of atmospheric blocking. *Geophysical Research Letters*, *31*, L06125. https://doi.org/10.1029/2003GL019341

Seneviratne, S. I., Corti, T., Davin, E. L., Hirschi, M., Jaeger, E. B., Lehner, I., et al. (2010). Investigating soil moisture-climate interactions in a changing climate: A review. *Earth-Science Reviews*, *99*(3–4), 125–161. https://doi.org/10.1016/j.earscirev.2010.02.004

Sillmann, J., Kharin, V. V., Zhang, X., Zwiers, F. W., & Bronaugh, D. (2013). Climate extremes indices in the CMIP5 multimodel ensemble: Part 1. Model evaluation in the present climate. *Journal of Geophysical Research: Atmospheres*, *118*, 1716–1733. https://doi.org/10.1002/jgrd.50203

Sousa, P. M., Trigo, R. M., Barriopedro, D., Soares, P. M. M., Ramos, A. M., & Liberato, M. L. R. (2017). Responses of European precipitation distributions and regimes to different blocking locations. *Climate Dynamics*, *48*(3–4), 1141–1160. https://doi.org/10.1007/s00382-016-3132-5

Sousa, P. M., Trigo, R. M., Barriopedro, D., Soares, P. M. M., & Santos, J. A. (2018). European temperature responses to blocking and ridge regional patterns. *Climate Dynamics*, *50*(1–2), 457–477. https://doi.org/10.1007/s00382-017-3620-2

Sprenger, M., Fragkoulidis, G., Binder, H., Croci-Maspoli, M., Graf, P., Grams, C. M., et al. (2017). Global climatologies of Eulerian and Lagrangian flow features based on ERA-Interim reanalyses. *Bulletin of the American Meteorological Society*, *98*, 1739–1748. https://doi.org/10.1175/BAMS-D-15-00299.1

Trigo, R. M., Trigo, I. F., DaCamara, C. C., & Osborn, T. J. (2004). Climate impact of the European winter blocking episodes from the NCEP/NCAR Reanalyses. *Climate Dynamics*, *23*(1), 17–28. https://doi.org/10.1007/s00382-004-0410-4

Wernli, H., & Schwierz, C. (2006). Surface cyclones in the ERA-40 dataset (1958–2001). Part I: Novel identification method and global climatology. *Journal of the Atmospheric Sciences*, *63*(10), 2486–2507. https://doi.org/10.1175/JAS3766.1

Whan, K., Zwiers, F., & Sillmann, J. (2016). The influence of atmospheric blocking on extreme winter minimum temperatures in North America. *Journal of Climate*, *29*(12), 4361–4381. https://doi.org/10.1175/JCLI-D-15-0493.1

Wilks, D. S. (2016). "The stippling shows statistically significant grid points": How research results are routinely overstated and overinterpreted, and what to do about it. *Bulletin of the American Meteorological Society*, *97*(12), 2263–2273. https://doi.org/10.1175/BAMS-D-15-00267.1

Woollings, T., Barriopedro, D., Methven, J., Son, S.-W., Martius, O., Harvey, B., et al. (2018). Blocking and its response to climate change. *Current Climate Change Reports*, *4*(3), 287–300. https://doi.org/10.1007/s40641-018-0108-z

Xu, K., Lu, R., Kim, B.-J., Park, J.-K., Mao, J., Byon, J.-Y., et al. (2019). Large-scale circulation anomalies associated with extreme heat in South Korea and southern–central Japan. *Journal of Climate*, *32*(10), 2747–2759. https://doi.org/10.1175/JCLI-D-18-0485.1

Zscheischler, J., & Seneviratne, S. I. (2017). Dependence of drivers affects risks associated with compound events. *Science Advances*, *3*(6), e1700263. https://doi.org/10.1126/sciadv.1700263

Zschenderlein, P., Fragkoulidis, G., Fink, A. H., & Wirth, V. (2018). Large-scale Rossby wave and synoptic-scale dynamic analyses of the unusually late 2016 heatwave over Europe. *Weather*, *73*(9), 275–283. https://doi.org/10.1002/wea.3278